Check for updates

# Circularly polarized luminescence and high photoluminescence quantum yields from rigid 5,10-dihydroindeno[2,1-*a*]indene and 2,2′-dialkoxy-1,1′-binaphthyl conjugates and copolymers†

Keisuke Iwata,[a] Makoto Tsurui,[b] Kosuke Itaya,[b] Naoto Hamaguchi,[a] Yasunobu Egawa,[a] Yuichi Kitagawa, [ID][b] Yasuchika Hasegawa [ID][b] and Hayato Tsuji [ID] *[a]

5,5,10,10-Tetramethyl-5,10-dihydroindeno[2,1-*a*]indene (COPV1(Me)) was installed into either the 3,3′- or 6,6′-positions of chiral 2,2′-dioctyloxy-1,1′-binaphthyl to afford 2 : 1 conjugates (monomeric compounds) and 1 : 1 copolymers. These compounds showed high photoluminescence quantum yields of >0.95 whilst also exhibiting circular dichroism (CD) and circularly polarized luminescence (CPL). The dissymmetry factors of CPL ($g_{CPL}$) for the 3,3′- and 6,6′-monomeric compounds in THF were $6.6 \times 10^{-4}$ and $3.3 \times 10^{-4}$, respectively. The 3,3′-isomer has a higher $g$ value than the 6,6′-isomer, which was attributed to the difference in the extent of π-conjugation and the angle between electronic and magnetic transition moments. The $g_{CPL}$ values of the 3,3′-linked and 6,6′-linked copolymers were $1.1 \times 10^{-3}$ and $6.8 \times 10^{-4}$, respectively. The structural rigidity of the COPV units is beneficial to achieve relatively high $g$ values whilst maintaining a photoluminescence quantum yield that is close to unity by using a single type of fluorophore.

## Introduction

Circularly polarized luminescence (CPL) has attracted much attention in recent years due to its broad range of applications in areas such as three-dimensional optical displays, optical sensors, and chiroptical switches.[1] CPL properties are commonly evaluated through the dissymmetry factor ($g_{CPL}$), which is defined as $4|m||\mu|\cos\theta/(|m|^2+|\mu|^2)$, where $m$ is the transition magnetic dipole moment, $\mu$ is the transition electronic dipole moment, and $\theta$ is the angle between these two vectors. Thus, $g_{CPL}$ is approximately proportional to $|m|/|\mu|$ assuming that $|m| << |\mu|$, and accordingly, there is usually a trade-off between $g_{CPL}$ and the photoluminescence quantum yield ($\Phi_{PL}$). Recent advances have enabled the synthesis of materials with both high $g_{CPL}$ and $\Phi_{PL}$. These materials have used molecular designs that conjugate fluorophores with cyclophane,[2] binaphthyl,[3] or other chiral scaffolds,[4] construct

chiral fluorophore frameworks based on helical,[5] spiro,[6] or cyclic[7] structures, or that complex with lanthanoids.[8] These design strategies have provided clues to the design principles underlying such materials.[9]

We have previously reported carbon-bridged oligo(phenylenevinylene)s (COPVs), which exhibit high photoluminescence (PL) efficiencies close to unity owing to their rigid planar phenylenevinylene structures that have intramolecular cross links with sp³-hybridized methylene groups.[10–13] We envisaged that this rigid extended π-conjugation skeleton would be beneficial to construct a large dissymmetric field with maintaining high $\Phi_{PL}$. Based on this strategy, we have prepared COPV derivatives that contain a binaphthyl group,[14,15] which is frequently used as a chiral scaffold for CPL molecules. Here, we report the synthesis and CPL properties of 2 : 1 conjugates (herein called monomeric compounds) of 5,5,10,10-tetramethyl-5,10-dihydroindeno[2,1-*a*]indene (COPV1) and 2,2′-dioctyloxy-1,1′-binaphthyl. The alternating copolymers showed $g_{CPL}$ values of up to $1.1 \times 10^{-3}$ with high fluorescence quantum yields (>0.95) by using a single type of fluorophore.

*[a]Department of Chemistry, Faculty of Science, Kanagawa University, 3-27-1 Rokkaku-bashi, Kanagawa-ku, Yokohama 221-8686, Japan. E-mail: tsujiha@kanagawa-u.ac.jp*

*[b]Faculty of Engineering, Hokkaido University, Kita13 Nishi8, Kita-ku, Sapporo 060-8628, Japan*

† Electronic supplementary information (ESI) available: ¹H and ¹³C NMR spectra of new compounds, computational calculation details of the model compounds. See DOI: https://doi.org/10.1039/d4ra00380b
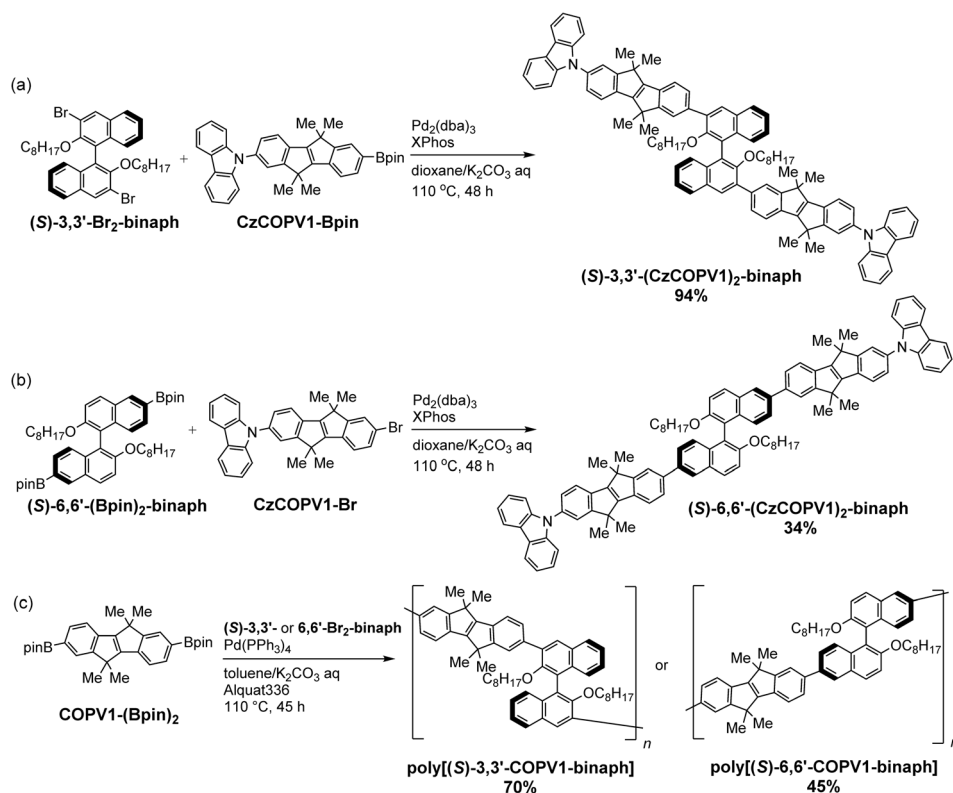
## Results and discussion

### Synthesis

The structures of the compounds used in the present study and their synthesis are shown in Scheme 1. Suzuki–Miyaura

**Scheme 1** Synthesis of COPV1-binaphthyl conjugates and co-polymers *via* Suzuki–Miyaura coupling. (a) (*S*)-3,3′-(CzCOPV1)$_2$-binaph, (b) (*S*)-6,6′-(CzCOPV1)$_2$-binaph, and (c) poly[(*S*)-3,3′-COPV1-binaph] and poly[(*S*)-6,6′-COPV1-binaph]

coupling of the COPV1 (ref. 12) and 2,2′-dioctyloxy-1,1′-binaphthyl units afforded the monomeric compounds (*S*)-3,3′-(CzCOPV1)$_2$-binaph and (*S*)-6,6′-(CzCOPV1)$_2$-binaph in 94% and 34% yield, respectively. Structures of the products were characterized using $^1$H and $^{13}$C NMR spectroscopy as well as mass spectrometry. Alternating (1 : 1) copolymers of COPV1 and 2,2′-dioctyloxy-1,1′-binaphthyl, *i.e.*, poly[(*S*)-3,3′-COPV1-binaph] and poly[(*S*)-6,6′-COPV1-binaph], were obtained in 70% and 45% yield, respectively. The average molecular weights $M_n$ and $M_w$ of these polymers were estimated by analytical gel-permeation chromatography (GPC) using polystyrene standards. The values for the 3,3′-polymer were $M_n = 8076$ and $M_w = 9839$ (PDI = 1.21) and those for the 6,6′-polymer $M_n = 9070$ and $M_w = 15$ 988 (PDI = 1.76). These molecular weights correspond to 11–12 repeating COPV1-binaph units.

## Calculations

Structural and CD/CPL parameter of the monomeric compounds were estimated by calculations on model compounds [(*S*)-3,3′-(COPV1)$_2$-binaph]′ and [(*S*)-6,6′-(COPV1)$_2$-binaph]′, which contain methoxy groups at the 2 and 2′ positions instead of octyloxy groups (Fig. S15† and Table 1). The dihedral angle between the two naphthyl groups ($\omega_1$) of the 6,6′-isomer in the ground state is 89.3°, which is a typical value for binaphthyl derivatives, while that of the 3,3′-isomer is 111.6° due to the steric repulsion between two COPV1 moieties. The dihedral angle between the naphthyl group and the COPV1

moiety ($\omega_2$) is 44.3° for the 3,3′-isomer and 36.1° for the 6,6′-isomer, suggesting more extension of the π-conjugation in the latter. Indeed, the Kohn–Sham orbitals suggest that the HOMO and HOMO−1 of the 6,6′-isomer are delocalized over the binaphthyl and COPV1 moieties, while the coefficients on the binaphthyl moiety are smaller in the 3,3′-isomer (Fig. 1). The LUMO and LUMO+1 of both compounds show large coefficients both in the binaphthyl and the COPV1 moieties.

As expected, relatively large rotatory strength velocity values were obtained for both the absorption and emission processes in both 3,3′- and 6,6′-isomers compared to reported compounds,[3i] indicating that dissymmetry fields are effectively constructed by connecting rigid COPV. Details of the excited-state geometries and the CD/CPL calculations will be discussed later.

## Absorption and PL spectra

The upper panels of Fig. 2 show the absorption and PL spectra of the two monomeric compounds and their respective copolymers measured in THF at room temperature. The related photophysical data are summarized in Table 2. (*S*)-3,3′-(CzCOPV1)$_2$-binaph and (*S*)-6,6′-(CzCOPV1)$_2$-binaph showed absorption maxima at 358 nm ($\varepsilon$ 8.85 × 10$^4$ M$^{-1}$ cm$^{-1}$) and 365 nm($\varepsilon$ 12.0 × 10$^4$ M$^{-1}$ cm$^{-1}$), respectively. The 6,6′-isomer has a longer absorption wavelength and higher extinction coefficient than its 3,3′-counterpart. This experimental finding can be rationalized in terms of the smaller twist angle between the

**Table 1** Summary of the calculations on the model compounds [(S)-3,3′-(COPV1)$_2$-binaph]′ and [(S)-6,6′-(COPV1)$_2$-binaph]′ [a]

| Model compound | State (configuration) | $d_{c-c}$[b]/Å | $d_{e-e}$[b]/Å | $\omega_1$[c]/° | $\omega_2$[c]/° | RS[d]/10$^{-40}$ erg esu cm Gauss$^{-1}$ | $\lvert\mu\rvert$[e]/10$^{-20}$ esu cm | $\lvert m\rvert$[e]/10$^{-20}$ erg Gauss$^{-1}$ | $\theta$[e]/° | $g$[f]/10$^{-4}$ |
|---|---|---|---|---|---|---|---|---|---|---|
| [(S)-3,3′-(COPV1)$_2$-binaph]′ | S$_0$ | 15.9 | 8.4 | 111.6 | 44.3 | 234 | 956 | 2.9 | 85.05 | 10.5 |
| | S$_1$ (HOMO → LUMO, HOMO−1 →LUMO+1) | 16.1 | 8.4 | 114.6 | 33.4 | 185 | 948 | 2.3 | 85.20 | 8.3 |
| [(S)-6,6′-(COPV1)$_2$-binaph]′ | S$_0$ | 18.2 | 10.3 | 89.3 | 36.1 | 146 | 1168 | 2.3 | 86.86 | 4.4 |
| | S$_1$ (HOMO−1 → LUMO, HOMO → LUMO+1) | 16.7 | 10.1 | 84.1 | 19.0, 36.0 | 72 | 1118 | 2.4 | 88.40 | 2.4 |

[a] Geometry-optimization calculations on the ground and excited states and TD DFT calculations to estimate CD and CPL characteristics were performed at the B3LYP/6–31g(d) level. [b] $d_{c-c}$: Center-to center (center of the vinylene moiety of the COPV1 unit with red markers in Fig. S15) distance between the COPV1 units. $d_{e-e}$: Edge-to-edge (carbon atoms with blue makers in Fig. S15 that are connected to the binaphthyl unit) distance between the COPV1 units. [c] $\omega_1$: Dihedral angles C2–C1–C1′–C2′, $\omega_2$: dihedral angles between the COPV1 and the naphthalene units of the binaphthyl moiety. [d] Rotatory strength velocity. [e] $\mu$: Transition electronic dipole moment; $m$: transition magnetic dipole moment; $\theta$: angle between these two vectors. [f] Dissymmetry factor calculated using the approximation $4\lvert m\rvert\cos\theta/\lvert\mu\rvert$.



**[(S)-3,3'-(COPV1)$_2$-binaph]′**    **[(S)-6,6'-(COPV1)$_2$-binaph]′**
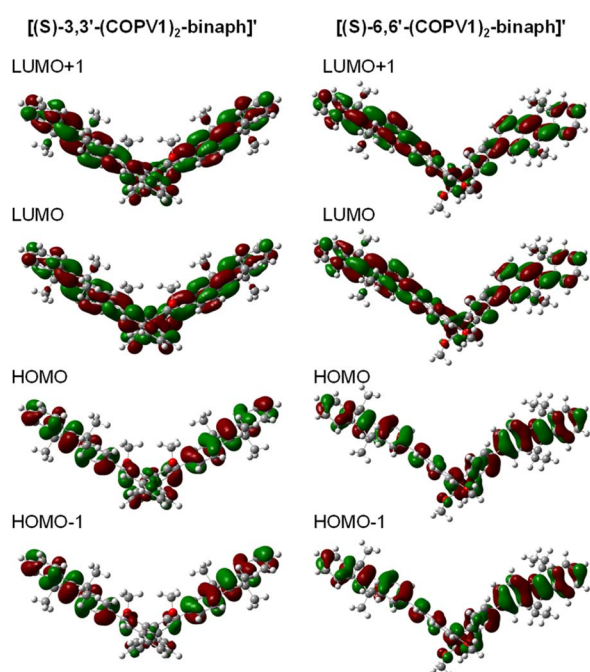
LUMO+1

LUMO

HOMO

HOMO−1

**Fig. 1** Molecular orbitals of model compounds [(S)-3,3′-(COPV1)$_2$-binaph]′ and [(S)-6,6′-(COPV1)$_2$-binaph]′ (view from the binaphthyl axis direction).

COPV and naphthalene units in the 6,6′-isomer and the difference of the distribution of HOMO and HOMO−1, which participate in the transition, as suggested by calculations on the model compounds (Table 1 and Fig. 1). The PL peaks appeared at 424 nm and 411 nm for the 3,3′- and 6,6′-isomers, respectively, with a moderate Stokes shift. The PL quantum yields were close to unity ($\Phi_{PL}$ > 0.95 for both compounds) owing to the structural rigidity of the COPV units. The polymers, poly[(S)-3,3′-COPV1-binaph] and poly[(S)-6,6′-COPV1-binaph], exhibited slightly red-shifted absorption (365 and 377 nm) and emission (417 and 425 nm) bands with respect to their monomeric counterparts. This is due to the almost orthogonal configuration about the binaphthyl axis, which suppresses the extension of conjugation. The PL quantum yields remained high (>0.95) for both polymers.

Fluorescence-lifetime measurements revealed very short emission lifetimes (∼1 ns) for the monomeric compounds and even shorter lifetimes for the polymers. The estimated radiative rate constants $k_r$ of the 3,3′- and 6,6′-monomeric compounds were $8.3 \times 10^8$ and $9.1 \times 10^8$ s$^{-1}$, respectively, both values being larger than that of COPV1 ($4.9 \times 10^8$ s$^{-1}$). This suggests the presence of extended π-conjugation *via* connection of the naphthalene and carbazole units to the COPV core. The $k_r$ values for the polymers were on the order of 10$^9$ s$^{-1}$, which is quite high for a series of COPV-based polymers,[11b,13] and thus this feature may be valuable for applications in CPL lasers.[3d]

### Circular dichroism (CD) and CPL

The CD and CPL spectra measured in THF at room temperature are shown in the lower panels of Fig. 2 and the accompanying data are summarized in Table 2. The CD spectra of the four compounds showed a positive Cotton effect, consistent with their absolute configuration and the twist angles between the two naphthalene units along the 1,1′-axis.[14–16] A comparison of the two monomeric compounds shows the 3,3′-isomer has a higher $g_{CD}$ value ($8.5 \times 10^{-4}$) than its 6,6′-counterpart ($4.3 \times 10^{-4}$). This can be understood from the optimized geometries in the ground state (Table 1). The 3,3′-isomer has a shorter distance between the two COPV chromophores with a center-to-center distance between the two COPV units of 15.9 Å and 18.2 Å for the 3,3′-isomer and the 6,6′-isomer, respectively.

The optimized geometries in the S$_1$ state showed small geometrical changes relative to the S$_0$ state. For example, the dihedral angle of the 3,3′-isomer only slightly changed from 111.6° (S$_0$) to 114.6° (S$_1$), and in the 6,6′-isomer it changed from 89.3° (S$_0$) to 84.1° (S$_1$). Despite these changes, the two COPV chromophores in the 3,3′-isomer are also closer in the S$_1$ state than those in the 6,6′-isomer. This leads to a similar trend for the $g_{CPL}$ values in the ground state where $g_{CPL} = 6.6 \times 10^{-4}$ for the 3,3′-monomer and $3.3 \times 10^{-4}$ for the 6,6′-monomer in THF, values which are higher than those of a compound with a similar fluorophore.[6] The CPL brightness value, $B_{CPL}$, (defined as $\varepsilon \times g_{CPL} \times \Phi_{PL}/2$)[17] for the 3,3′-monomer was 28, which is
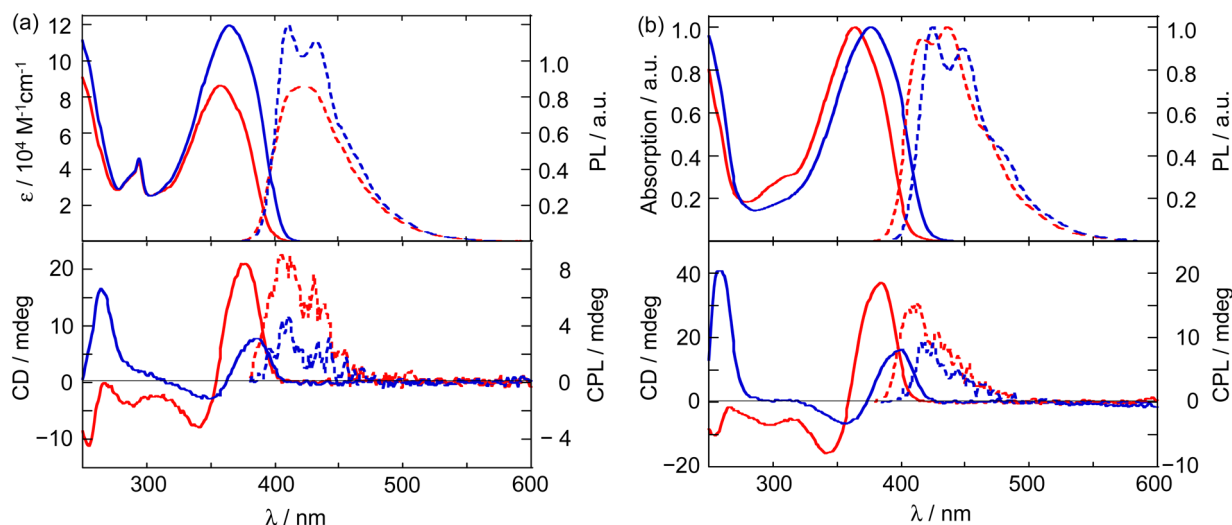
**Fig. 2** Photophysical properties in THF at room temperature. Top: absorption spectra (solid lines) and photoluminescence spectra (dashed lines). Bottom: CD (solid lines) and CPL (dashed lines) spectra. (a) Monomeric compounds (red: (S)-3,3′-(CzCOPV1)$_2$-binaph and blue: (S)-6,6′-(CzCOPV1)$_2$-binaph) and (b) polymers (red: poly[(S)-3,3′-COPV1-binaph] and blue: poly[(S)-6,6′-COPV1-binaph]).

**Table 2** Summary of the photophysical properties in THF at room temperature[a]

| Compound | $\lambda_{abs}$/nm | $\varepsilon$/10$^4$ L mol$^{-1}$ cm$^{-1}$ | $g_{CD}$/10$^{-4}$ | $\lambda_{PL}$/nm | $\Phi_{PL}$ | $\tau^b$/ns | $k_r^c$/10$^8$ s$^{-1}$ | $k_{nr}^c$/10$^8$ s$^{-1}$ | $g_{CPL}$/10$^{-4}$ | $B_{CPL}$/M$^{-1}$ cm$^{-1}$ |
|---|---|---|---|---|---|---|---|---|---|---|
| (S)-3,3′-(CzCOPV1)$_2$-binaph | 358 | 8.85 | 8.5 (377 nm) | 424 | >0.95 | 1.15 | 8.3 | 0.34 | 6.6 (406 nm) | 28 |
| (S)-6,6′-(CzCOPV1)$_2$-binaph | 365 | 12.0 | 4.3 (390 nm) | 411, 433 | >0.95 | 1.05 | 9.1 | 0.38 | 3.3 (406 nm) | 19 |
| poly[(S)-3,3′-COPV1-binaph] | 365 | | 15 (384 nm) | 417, 436 | >0.95 | 0.94 | 10.3 | 0.32 | 11 (413 nm) | |
| poly[(S)-6,6′-COPV1-binaph] | 377 | | 7.5 (401 nm) | 425, 449 | >0.95 | 0.86 | 10.2 | 0.35 | 6.8 (419 nm) | |

[a] Standard error: $\lambda_{abs}$ and $\lambda_{PL}$: <±1 nm; $\varepsilon$: ±2%; $\Phi_{PL}$: ±5%. [b] Fluorescence lifetime ($\tau$) under excitation from a 365 nm LED. [c] Radiative decay constant ($k_r$) and non-radiative decay constant ($k_{nr}$) calculated using $\Phi$ and $\tau$.

higher than that of the 6,6′-isomer (19). These $B_{CPL}$ values are modest for binaphthyl-based CPL compounds.[3,17]

More insights into the $g$ values were obtained from calculations on the monomeric model compounds (Tables 1 and 2). These calculations revealed that the smaller $g$ values of the 6,6′-isomer can be attributed to two main factors when compared to those of the 3,3′-isomer.[3d-f] Firstly, the electronic transition moment ($|\mu|$) of the 6,6′-isomer is higher than that of the 3,3′-isomer, reflecting the differences with respect to the extent of π-conjugation. Nevertheless, it is noteworthy that the 3,3′-isomer keeps high PLQY of >0.95 by taking advantage of the rigidity of the COPV fluorophore. Secondly, the angles ($\theta$) between the vectors of the electronic and the magnetic transition moment of the 6,6′-isomer are closer to 90° (86.86° and 88.40°) than those of the 3,3′-isomer (85.05° and 85.20°). In any case, these are all close to 90°, which is detrimental to achieving high $g$-values and will need to be addressed by a more appropriate molecular design in the near future. The smaller $g$ values in CPL compared to those in CD is a common phenomenon for both isomers, while the origin seems to be different for each isomer. For the 3,3′-isomer, the magnetic transition moment ($|m|$) for the CPL is smaller than that of CD. Meanwhile, in the 6,6′-isomer, the $\theta$ value increases from 86.86° (CD) to 88.40° (CPL) without significant change of the $|\mu|$ and $|m|$ values.

The $g$ values of the 6,6′-polymer ($g_{CD}$ = 5.6–7.5 × 10$^{-4}$; $g_{CPL}$ = 6.8 × 10$^{-4}$) are slightly higher than those of the corresponding monomeric compounds, and those of the 3,3′-polymer reached an order of magnitude of 10$^{-3}$ in both the CD and CPL measurements in THF ($g_{CD}$ = 1.5–1.6 × 10$^{-3}$; $g_{CPL}$ = 1.1 × 10$^{-3}$). The experimental results suggesting that the 3,3′-polymer has higher dissymmetric factors than the 6,6′-polymer are corroborated by theoretical calculations (Fig. S16†), which suggest that the 3,3′-polymer more efficiently forms a helical structure with a smaller pitch.

## Experimental

### Instruments

Proton nuclear magnetic resonance ($^1$H NMR) spectra were recorded using JEOL ECA-400 (400 MHz), ECS-400 (400 MHz), or ECZ-600 (600 MHz) spectrometers. Chemical shift data for the protons are reported in parts per million (ppm, $\delta$ scale) downfield from tetramethylsilane and are referenced to the residual protons in the NMR solvent (C$_6$D$_6$: $\delta$ 7.20). Carbon nuclear magnetic resonance spectra ($^{13}$C NMR) were recorded at 150 MHz and the chemical data for the carbons are reported in parts per million (ppm, $\delta$ scale) downfield from tetramethylsilane and referenced to the carbon resonance of the solvent (C$_6$D$_6$:

$\delta$ 128.00). The data are presented as follows: chemical shift, multiplicity ($s$ = singlet, $d$ = doublet, $t$ = triplet, $m$ = multiplet), coupling constant in hertz (Hz), and integration. Preparative gel-permeation column chromatography (GPC) was performed on a Japan Analytical Industry LaboACE LC-5060 (eluent: chloroform) with JAIGEL 2HR and 2.5HR.

### Synthesis of (S)-3,3′-(CzCOPV1)$_2$-binaph

A mixture of CzCOPV1-Bpin (27.4 mg, $5.00 \times 10^{-2}$ mmol), (S)-3,3′-Br$_2$-binaph (15.3 mg, $2.29 \times 10^{-2}$ mmol), and Pd(PPh$_3$)$_4$ (3.5 mg, $3.03 \times 10^{-3}$ mmol) in toluene (1.3 mL) with 2 M aqueous K$_2$CO$_3$ solution (1 mL) was stirred at 110 °C for 69 h. The reaction mixture was diluted with dichloromethane and passed through a short plug of silica gel. The solvent was removed *in vacuo*. The crude mixture was subjected to preparative GPC (eluent: THF). Further purification was performed by preparative thin-layer chromatography (TLC) developed with hexane/CH$_2$Cl$_2$ = 2/1 to give a pale yellow solid (29.2 mg, 94% yield). Mp > 300 °C. $^1$H NMR (400 MHz, C$_6$D$_6$ $\delta$ in ppm): 0.68–0.93 (m, 4H), 0.85 (t, $J$ = 7.2 Hz, 6H), 0.93–1.13 (m, 14H), 1.20 (q, $J$ = 7.2 Hz, 4H), 1.27–1.43 (m, 6H), 1.47 (s, 6H), 1.48 (s, 6H), 1.64 (s, 6H), 1.65 (s, 6H), 3.54–3.60 (m, 2H), 3.90–3.93 (m, 2H), 7.11–7.14 (m, 2H), 7.26–7.28 (m, 2H),7.29 (d, $J$ = 7.8 Hz, 4H), 7.31–7.35 (m, 4H), 7.39–7.41 (m, 6H), 7.49–7.51 (m, 6H), 7.58 (d, $J$ = 8.4 Hz, 2H), 7.92 (d, $J$ = 8.4 Hz, 2H), 7.98 (dd, $J$ = 1.8, 7.8 Hz, 2H), 8.19 (d, $J$ = 7.2 Hz, 4H), 8.27 (s, 2H), 8.33 (d, $J$ = 1.8 Hz, 2H). $^{13}$C{$^1$H} NMR (150 MHz, C$_6$D$_6$, $\delta$ in ppm): 14.2, 23.0, 24.4, 24.54, 24.58, 26.0, 29.5, 30.2, 30.5, 32.1, 45.4, 73.4, 110.2, 120.0, 120.3, 120.5, 120.8, 121.5, 123.9, 125.3, 126.2, 126.3, 126.54, 126.58, 130.8, 131.6, 134.5, 135.0, 136.5, 136.9, 137.2, 137.5, 141.9, 154.5, 155.8, 157.0, 159.3, 161.0 (some peaks overlap). HRMS (APCI+) $m/z$ calcd for C$_{100}$H$_{96}$N$_2$O$_2^+$([M$^+$]): 1356.7466, found: 1356.7491.

### Synthesis of (S)-6,6′-(CzCOPV1)$_2$-binaph

A mixture of Cz-COPV1-Br (25.0 mg, $4.96 \times 10^{-2}$ mmol), (S)-6,6′-(Bpin)$_2$-binaph (14.2 mg, $2.51 \times 10^{-2}$ mmol), Pd$_2$(dba)$_3$ (1.1 mg, $1.20 \times 10^{-2}$ mmol) and XPhos (1.2 mg, $2.52 \times 10^{-3}$ mmol) in 1,4-dioxane (1 mL) and 2 M aqueous K$_2$CO$_3$ solution (0.05 mL) was stirred at 110 °C for 48 h. The reaction mixture was diluted with dichloromethane and passed through a short silica gel plug. The solvent was removed *in vacuo*. The residue was subjected to preparative GPC (eluent: chloroform). Further purification with preparative TLC developed with hexane/CH$_2$Cl$_2$ = 2/1 gave a pale yellow solid (10.0 mg, 34% yield). Mp 169–171 °C (decomp). $^1$H NMR (400 MHz, CDCl$_3$ $\delta$ in ppm): 0.94 (t, $J$ = 7.2 Hz, 6H), 1.04–1.10 (m, 8H), 1.11–1.15 (m, 4H), 1.16–1.21 (m, 4H), 1.25–1.31 (m, 4H), 1.43–1.49 (m, 4H), 1.48 (brs, 12H), 1.607 (s, 6H), 1.612 (s, 6H), 3.88–3.92 (m, 2H), 3.95–3.99 (m, 2H), 7.28 (brd, $J$ = 7.8 Hz, 2H), 7.32 (s, $J$ = 7.8, 2H), 7.33–7.36 (m, 4H), 7.38–7.45 (m, 10H), 7.54 (d, $J$ = 8.4 Hz, 4H), 7.71 (d, $J$ = 8.4 Hz, 4H), 7.78 (d, $J$ = 8.4 Hz, 2H), 7.91 (s, 2H), 8.05 (d, $J$ = 8.4 Hz, 2H), 8.19 (d, $J$ = 7.2 Hz, 2H), 8.38 (s, 2H). $^{13}$C{$^1$H} NMR (150 MHz, CDCl$_3$, $\delta$ in ppm), 14.4, 23.1, 24.3, 24.6, 26.2, 29.5, 29.6, 29.8, 32.2, 45.6, 45.6, 69.5, 110.3, 116.1, 120.28, 120.33, 120.4, 120.8, 121.0, 121.48, 121.52, 124.0, 126.2, 126.3, 126.6, 126.8, 127.0, 129.8, 130.3, 134.2, 135.0, 136.9, 137.5, 137.6, 139.3, 141.9, 155.31, 155.36, 157.1, 160.0, 161.0

(some peaks overlap). HRMS (APCI+) $m/z$ calcd for C$_{100}$H$_{96}$N$_2$O$_2^+$([M$^+$]): 1356.7466, found: 1356.7518.

### Synthesis of poly[(S)-6,6′-COPV1-binaph]

A mixture of COPV1-(Bpin)$_2$ (50.4 mg, $9.84 \times 10^{-2}$ mmol), (S)-6,6′-Br$_2$-binaph (65.9 mg, $9.86 \times 10^{-2}$ mmol), Pd(PPh$_3$)$_4$ (22.7 mg, $1.96 \times 10^{-2}$ mmol), and a catalytic amount of Aliquat 336 (three drops) in toluene (2.5 mL) with 2 M aqueous K$_2$CO$_3$ solution (1.6 mL) was stirred at 110 °C for 24 h. An excess amount of iodobenzene was then added to the reaction mixture and stirred at 110 °C for 3 h. An excess amount of 4,4,5,5-tetramethyl-2-phenyl-1,3,2-dioxaborolane was added to the reaction, and the mixture was stirred at 110 °C for another 12 h. The reaction mixture was diluted with chloroform and passed over a short silica gel plug. The solvent was removed *in vacuo*. The crude mixture was subjected to preparative GPC (eluent: dichloroethane) to remove any small molecules. Further purification with preparative TLC developed with hexane/CH$_2$Cl$_2$ = 2/1 gave a yellow solid (34.2 mg, 45% yield). $^1$H NMR (600 MHz, C$_6$D$_6$ $\delta$ in ppm): 0.93 (t, $J$ = 7.2 Hz, 6H), 1.02–1.10 (m, 6H), 1.10–1.15 (m, 4H), 1.14–1.21 (m, 4H), 1.25–1.29 (m, 4H), 1.32–1.51 (m, 6H), 1.61 (s, 12H), 7.42–7.44 (m, 4H), 7.71–7.72 (m, 4H), 7.76 (d, $J$ = 8.4 Hz, 2H), 8.03 (d, $J$ = 9.0 Hz, 2H), 8.37 (s, 2H). $^{13}$C{$^1$H} NMR (150 MHz, C$_6$D$_6$, $\delta$ in ppm): 14.3, 23.0, 24.7, 26.2, 29.5, 29.6, 29.8, 32.1, 45.3, 69.5, 116.1, 120.1, 121.0, 121.4, 126.2, 126.5, 126.8, 129.1, 129.8, 130.3, 134.2, 137.3, 137.6, 138.9, 155.2, 156.1, 160.1. $M_n$: 9070, $M_w$: 15 988, $M_w/M_n$: 1.76.

### Poly[(S)-3,3′-COPV1(Me)-binaph]

Yellow solid (70%). $^1$H NMR (600 MHz, C$_6$D$_6$, $\delta$ in ppm): 0.6–0.9 (m, 6H), 0.84 (t, $J$ = 7.2 Hz, 3H), 0.9–1.1 (m, 12H), 1.16–1.21 (m, 4H), 1.24–1.33 (m, 2H), 1.64 (s, 6H), 1.65 (s, 6H), 3.54 (brs, 2H), 3.90 (brs, 2H), 7.09–7.11 (m, 2H), 7.27–7.29 (m, 2H), 7.50 (d, $J$ = 7.8 Hz, 2H), 7.56 (d, $J$ = 8.4 Hz, 2H), 7.89 (d, $J$ = 7.8 Hz, 2H), 7.94 (d, $J$ = 7.2 Hz, 2H), 8.24 (s, 2H), 8.29 (s, 2H). $^{13}$C{$^1$H} NMR (150 MHz, C$_6$D$_6$): 14.0, 22.6, 24.61, 24.65, 25.5, 29.0, 29.1, 29.9, 31.7, 45.1, 72.7, 119.0, 123.1, 124.6, 125.9, 126.0, 126.5, 127.7, 127.9, 128.46, 128.53, 130.1, 130.8, 131.9, 132.06, 132.12, 133.7, 135.8, 137.0, 153.7, 155.8, 158.8 (some peaks overlap). $M_n$: 8076, $M_w$: 9839, $M_w/M_n$: 1.21.

### Calculations

Geometry optimizations and TD DFT calculations were performed on the monomeric model compounds (S)-3,3′-(CzCOPV1)$_2$-binaph and (S)-6,6′-(CzCOPV1)$_2$-binaph at the B3LYP/6-31G(d) level in Gaussian 16. A frequency analysis was performed for each compound in order to confirm the absence of any imaginary frequency.

### Spectroscopy

UV/vis absorption spectra were measured on a JASCO V-770. Fluorescence spectra were measured on a JASCO FP-6500. Photoluminescence quantum yields (PLQY) were measured on a Hamamatsu Photonics C9920–02 Absolute PL Quantum Yield Measurement System, and absolute quantum yields were

determined using a calibrated integrating sphere system. Fluorescence lifetimes were estimated using the time-correlated single photon counting (TCSPC) operation mode on a Hamamatsu Photonics C11367-02. Both PLQY and lifetime measurements were performed using an excitation wavelength of 365 nm. CD and CPL spectra were recorded using a solution with 0.2 mg of solute in 10 mL of solvent on a JASCO J-1500 and CPL-300, respectively.

## Conclusions

We have demonstrated that the presence of structurally rigid and highly luminescent COPV units in chiral binaphthyl-COPV conjugates is beneficial for achieving $g$ values of an order of magnitude of up to $10^{-3}$ whilst maintaining a photoluminescence quantum yield of close to unity by using a single type of fluorophore. Similar to other fluorophores, the introduction of COPVs at the 3,3′-positions of binaphthyl, rather than at the 6,6′-positions, was more effective for exciton coupling, and thus for obtaining higher circular dichroism (CD) and circularly polarized luminescence (CPL) dissymmetric factors. The resulting $g$ values have remained in the early $10^{-3}$ range in the present work primarily because the angles $\theta$ between $m$ and $\mu$ vectors are all close to 90°. Nevertheless, by arranging the rigid COPV fluorophores appropriately to reduce $\theta$, it is expected that even higher $g$ values can be attained, considering that relatively large rotatory strengths were achieved even in the present form. Combining the properties presented here with the large radiative decay constants of up to an order of magnitude of $10^9$ s$^{-1}$, the present molecular and polymer designs could potentially be valuable in the field of CPL lasers, an area which we will focus on in the near future.

## Author contributions

Conceptualization, methodology, supervision and validation: YK, YH, HT; funding acquisition: YH, HT; investigation: KIw, MT, KIt, NH, YE; project administration: YH, HT; visualization: HT; writing-original draft: KIw, HT; writing-review and editing: YK, YH, HT.

## Conflicts of interest

There are no conflicts to declare.

## Acknowledgements

## Notes and references

1 (a) M. Li, Y. Wang, D. Zhang, L. Duan and C. Chen, *Angew. Chem., Int. Ed.*, 2020, **59**, 3500; (b) D. Zhang, M. Li and C. Chen, *Chem. Soc. Rev.*, 2020, **49**, 1331; (c) Y. Imai, Y. Nakano, T. Kawai and J. Yuasa, *Angew. Chem., Int. Ed.*, 2018, **57**, 8973; (d) J. Gong, M. Yu, C. Wang, J. Tan, S. Wang, S. Zhao, Z. Zhao, A. Qin, B. Tang and X. Zhang, *Chem. Commun.*, 2019, **55**, 10768; (e) J. Yan, F. Ota, B. A. San Jose and K. Akagi, *Adv. Funct. Mater.*, 2017, **27**, 1604529; (f) L. Zhang, H. Wang, S. Li and M. Liu, *Chem. Soc. Rev.*, 2020, **49**, 9095.

2 (a) Y. Morisaki, M. Gon, T. Sasamori, N. Tokitoh and Y. Chujo, *J. Am. Chem. Soc.*, 2014, **136**(9), 335; (b) Y. Morisaki, R. Sawada, M. Gon and Y. Chujo, *Chem.–An Asian J.*, 2016, **11**, 2524; (c) R. Sawada, M. Gon, J. Nakamura, Y. Morisaki and Y. Chujo, *Chirality*, 2018, **30**, 1109; (d) M. Zhang, X. Liang, D. Ni, D. Liu, Q. Peng and C. Zhao, *Org. Lett.*, 2021, **23**, 2; (e) Y. Sasai, R. Inoue and Y. Morisaki, *Bull. Chem. Soc. Jpn.*, 2020, **93**, 1193; (f) K. Ogawa, N. Miki, R. Inoue and Y. Morisaki, *ChemistrySelect*, 2023, **8**, e202301844.

3 (a) T. Amako, T. Kimoto, N. Tajima, M. Fujiki and Y. Imai, *Tetrahedron*, 2013, **69**, 2753; (b) Y. Kitayama, T. Amako, N. Suzuki, M. Fujiki and Y. Imai, *Org. Biomol. Chem.*, 2014, **12**, 4342; (c) J. Kumar, T. Nakashima, H. Tsumatori and T. Kawai, *J. Phys. Chem. Lett.*, 2014, **5**, 316; (d) J. Jiménez, L. Cerdán, F. Moreno, B. L. Maroto, I. García-Moreno, J. L. Lunkley, G. Muller and S. de la Moya, *J. Phys. Chem. C*, 2017, **121**, 5287; (e) S. Nakanishi, N. Hara, N. Kuroda, N. Tajima, M. Fujiki and Y. Imai, *Org. Biomol. Chem.*, 2018, **16**, 1093; (f) K. Takaishi, S. Murakami, K. Iwachido and T. Ema, *Chem. Sci.*, 2021, **12**, 14570; (g) Y. Wang, X. Li, L. Yang, W.-Y. Sun, C. Zhu and Y. Cheng, *Mater. Chem. Front.*, 2018, **2**, 554; (h) X. Zhang, Y. Zhang, H. Zhang, Y. Quan, Y. Li, Y. Cheng and S. Ye, *Org. Lett.*, 2019, **21**, 439; (i) X. Zhang, Y. Zhang, Y. Li, Y. Quan, Y. Cheng and Y. Li, *Chem. Commun.*, 2019, **55**, 9845; (j) M. Hasegawa, C. Hasegawa, Y. Nagaya, K. Tsubaki and Y. Mazaki, *Chem.–An Euro. J.*, 2022, **28**, e202202218; (k) K. Zhang, J. Zhao, N. Zhang, J.-F. Chen, N. Wang, X. Yin, X. Zheng and P. Chen, *J. Mater. Chem. C*, 2022, **10**, 1816; (l) M. Hasegawa, Y. Nojima, Y. Nagata, K. Usui, K.-I. Sugiura and Y. Mazaki, *Eur. J. Org Chem.*, 2023, **26**, e202300656.

4 H. Shigemitsu, K. Kawakami, R. Kajiwara, S. Yamada, T. Mori and T. Kida, *Angew. Chem., Int. Ed.*, 2022, **61**, e202114700.

5 (a) Y. Liu, Z. Wang and W. Jiang, *J. Am. Chem. Soc.*, 2022, **144**, 11397; (b) T. Otani, A. Tsuyuki, T. Iwachi, S. Someya, K. Tateno, H. Kawai, T. Saito, K. S. Kanyiva and T. Shibata, *Angew. Chem., Int. Ed.*, 2017, **56**, 3906; (c) H. Kubo, T. Hirose, T. Nakashima, T. Kawai, J. Hasegawa and K. Matsuda, *J. Phys. Chem. Lett.*, 2021, **12**, 686; (d) T. Cadart, D. Nečas, R. P. Kaiser, I. Favereau, I. Císařová, R. Gyepes, J. Hodačová, K. Kalíková, L. Bednárová, J. Crassous and M. Kotora, *Chem.–An Euro. J.*, 2021, **27**, 11279.

6 H. Hamada, Y. Itabashi, R. Shang and E. Nakamura, *J. Am. Chem. Soc.*, 2020, **142**, 2059.

7 (a) S. Sato, A. Yoshii, S. Takahashi, S. Furumi, M. Takeuchi and H. Isobe, *Proc. Natl. Acad. Sci.*, 2017, **114**, 13097; (b)

K. Sato, M. Hasegawa, Y. Nojima and N. Hara, *Chem.–An Euro. J.*, 2021, **27**, 1323.

8  (*a*) M. J. Islam, Y. Kitagawa, M. Tsurui and Y. Hasegawa, *Dalton Trans.*, 2021, **50**, 5433; (*b*) Y. Kitagawa, S. Wada, M. D. J. Islam, K. Saita, M. Gon, K. Fushimi, K. Tanaka, S. Maeda and Y. Hasegawa, *Commun. Chem.*, 2020, **3**, 119; (*c*) J. L. Lunkley, D. Shirotani, K. Yamanari, S. Kaizaki and G. Muller, *J. Am. Chem. Soc.*, 2008, **130**, 13814.

9  J.-M. Teng, D.-W. Zhang and C.-F. Chen, *ChemPhotoChem*, 2022, **6**, e202100228.

10  (*a*) H. Tsuji, *Bull. Chem. Soc. Jpn.*, 2022, **95**, 657; (*b*) H. Tsuji and E. Nakamura, *Acc. Chem. Res.*, 2019, **52**, 2939.

11  (*a*) X. Zhu, H. Tsuji, J. T. Lopez Navarrete, J. Casado and E. Nakamura, *J. Am. Chem. Soc.*, 2012, **134**, 19254; (*b*) M. Morales-Vidal, P. G. Boj, J. M. Villalvilla, J. A. Quintana, Q. Yan, N.-T. Lin, X. Zhu, N. Ruangsupapichat, J. Casado, H. Tsuji, E. Nakamura and M. A. Díaz-García, *Nat. Commun.*, 2015, **6**, 8458.

12  K. Iwata, Y. Egawa, K. Yamanishi and H. Tsuji, *J. Org. Chem.*, 2022, **87**, 13882.

13  (*a*) H. Nishioka, H. Tsuji and E. Nakamura, *Macromolecules*, 2018, **51**, 2961; (*b*) M. Morales-Vidal, J. A. Quintana, J. M. Villalvilla, P. G. Boj, H. Nishioka, H. Tsuji, E. Nakamura, G. L. Whitworth, G. A. Turnbull, I. D. W. Samuel and M. A. Díaz-García, *Adv. Opt. Mater.*, 2018, **6**, 1800069.

14  For recent examples, see:(*a*) T. Kimito, N. Tajima, M. Fujiki and Y. Imai, *Chem.–An Asian J.*, 2012, **7**, 2836; (*b*) T. Kinuta, N. Tajima, M. Fujiki, M. Miyazawa and Y. Imai, *Tetrahedron*, 2012, **68**, 4791.

15  Reviews:(*a*) L. Pu, *Chem. Rev.*, 1998, **98**, 2405; (*b*) Y. Imai, *J. Jpn. Soc. Colour Mater.*, 2015, **88**, 383.

16  (*a*) N. Berova, L. Di Bari and G. Pescitelli, *Chem. Soc. Rev.*, 2007, **36**, 914; (*b*) L. Di Bari, G. Pescitelli and P. Salvadori, *J. Am. Chem. Soc.*, 1999, **121**, 7998; (*c*) S. F. Mason, R. H. Seal and D. R. Roberts, *Tetrahedron*, 1974, **30**, 1671; (*d*) I. Hanazaki and H. Akimoto, *J. Am. Chem. Soc.*, 1972, **94**, 4102.

17  L. Arrico, L. Di Bari and F. Zinna, *Chem.–An Euro. J.*, 2021, **27**, 2920.